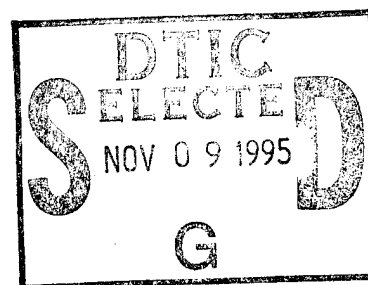


NATIONAL AIR INTELLIGENCE CENTER



RESEARCH ON THE CHARACTERISTICS OF DYNAMIC PYROLYSIS
AND THE KINETICS OF CYCLIZATION FOR PAN FIBERS USING
IN SITU X-RAY DIFFRACTION TECHNIQUES



Approved for public release:
distribution unlimited

DTIC QUALITY INSPECTED B

19951108 031

HUMAN TRANSLATION

NAIC-ID(RS)T-0278-95 19 October 1995

MICROFICHE NR: 95C000655

RESEARCH ON THE CHARACTERISTICS OF DYNAMIC PYROLYSIS
AND THE KINETICS OF CYCLIZATION FOR PAN FIBERS USING
IN SITU X-RAY DIFFRACTION TECHNIQUES

English pages: 15

Source: Gaofenzi Xuebao, Nr. 5, October 1993;
pp. 549-555

Country of origin: China

Translated by: SCITRAN
F33657-84-D-0165

Requester: NAIC/TATV/Robert M. Dunco

Approved for public release: distribution unlimited.

THIS TRANSLATION IS A RENDITION OF THE ORIGINAL FOREIGN TEXT WITHOUT ANY ANALYTICAL OR EDITORIAL COMMENT STATEMENTS OR THEORIES ADVOCATED OR IMPLIED ARE THOSE OF THE SOURCE AND DO NOT NECESSARILY REFLECT THE POSITION OR OPINION OF THE NATIONAL AIR INTELLIGENCE CENTER.

PREPARED BY:

TRANSLATION SERVICES
NATIONAL AIR INTELLIGENCE CENTER
WPAFB, OHIO

ABSTRACT

This article uses in situ X ray diffraction techniques to study PAN (polyacrylonitrile) preoxidation processes. In a series of resolution charts obtained from wide angle measurements and varying with sample pyrolysis times at different temperatures, calculations are made of sample crystallinities, microcrystalline dimensions, crystal lattice spacing, and "aromatization" indices. In conjunction with this, explanations are given for the transient cases associated with these parameters following along with changes in experimental conditions. At the same time, descriptions are also done of cyclization kinematics behavior associated with PAN fibers during preoxidation processes. Solutions are made for cyclization reaction speeds and activation parameters at various temperatures.

KEY WORDS PAN fiber, Pyrolytic characteristics, Kinetics of cyclization, In situ X ray diffraction techniques

Accession For	
NTIS CRA&I	<input checked="" type="checkbox"/>
DTIC TAB	<input type="checkbox"/>
Unannounced	<input type="checkbox"/>
Justification	
By	
Distribution /	
Availability Codes	
Dist	Avail and/or Special
A-1	

GRAPHICS DISCLAIMER

All figures, graphics, tables, equations, etc. merged into this translation were extracted from the best quality copy available.

Following along with the break neck development of materials science, which is one of the three great pillars of modern civilization, carbon fibers, which have prospects in national economies and the peoples' livelihood, have received a high degree of serious attention from the scientists and entrepreneurs of various countries. In particular, broad research [1-4] has been carried out on one of the raw materials taken to make carbon gauze--thermal dissociated PAN fibers. Option is made for in situ techniques in order to track changes in system constituent structures. Although there are incomparable advantages, making use of in situ X ray diffraction methods on PAN fiber pyrolysis processes to carry out tracking has, however, been reported up to now in very few references.

In order to better observe dynamic changes during PAN fiber low temperature pyrolysis processes, this article uses in situ X ray diffraction techniques to study PAN fiber transient dynamic pyrolysis characteristics, tracking structural changes generated by samples in pyrolysis periods and thereby obtaining structural details better able to reflect serial patterns of transient change behaviors and to use structural changes in order to show signs of the kinetic course of nitrile radical cyclization in PAN.

* Numbers in margins indicate foreign pagination.
Commas in numbers indicate decimals.

EXPERIMENTAL SECTION

1. Samples

The samples used in this article were supplied by the Jilin chemical industry company reagent plant. The PAN fiber bundles in question are 1000 fibers to a bundle. Their characteristics are a fiber size (fiber unit), strength (gram/fiber unit), and elongation (%) of 1.10, 4.57, and 14.60 respectively. In fibers, the contained amounts of carbon, hydrogen, nitrogen, and oxygen (wt%) are respectively 65.56, 5.76, 24.51, and 2.77.

2. Instrumentation and Experimental Conditions

/550

Experiments were carried out on a 2311B1 high temperature apparatus associated with a Japanese scientific D/max-rA 12kw revolving target anode X ray diffraction instrument. Apparatus control systems indicate temperatures and make use beforehand of standard thermocouples to carry out calibration. Taking fiber samples in strictly parallel arrangements, they are put onto the sample platform in a platinum wire electric furnace, and temperature control thermocouples are fixed to the side surfaces of samples. Following that, by computer, temperature settings are raised in accordance with setting sequence speeds of 20°C/min up to preset temperatures. Beginning with each interval associated with a certain time period (or temperature), one iteration of X ray diffraction scanning is carried out. The scanning range is 2θ from 12° to 32°. X ray test samples

are dynamically measured in an air atmosphere. Diffraction conditions are: Cu target radiation sources; graphite monochromators; tube voltages of 40 thousand volts, tube currents of 80 milliamperes; incidence slit 1° , receiver slit 0.4mm, scattering slit 1.2° . Use was made of fixed time stepped scanning methods to collect data. Step width was 0.02° . Time was 0.5 seconds.

RESULTS AND DISCUSSION

1. Patterns of PAN Fiber Structures in Air Atmosphere Following Along with Changes in Pyrolysis Temperatures and Times

From Fig.1, it is possible to know that, at a $2\theta=16.16^\circ$ location, there is a very strong diffraction peak (100 surface). It is a reflection of molecular bond spacing in molecule segments. At a $2\theta=28.67^\circ$ location, there is another relatively weak diffraction peak (110 surface). It reflects the distance between molecular sections which are nearly parallel [5]. This type of two tiered diffraction characteristic represents relatively high lateral serial pattern structures possessed by the samples in question. It matches up with results reported by such people as Wegener [6] and Gupta [7]. At the same time, in charts, it is also clearly shown that there exists between these two diffraction peaks a broad area of diffused reflection, clearly showing unordered phases spread all over through the entire structure in unseparated modes [8].

When the samples in question are continuously heated in air- -before 195°C --the diffraction strengths do not greatly

change. After 195°C, there is then an obvious drop. Moreover, at a $2\theta=24.78^\circ$ location, one has the appearance of a new (101) diffraction peak. When temperatures rise to 250°C, (110) peaks have already basically disappeared. Moreover, (100) peak diffraction strengths diminish very, very greatly, and peak forms become wide and diffuse, as well as (101) peak strengths obviously increasing. This means nothing else than that the molecular bonds associated with acrylonitrile structures in fibers--given rise to because of temperatures in the systems in question--have been destroyed. A drop in crystal formation is created, leading to a change to smaller microcrystal sizes. At the same time, acrylonitrile elements at locations on the edges of fiber molecules begin to form polyamide trapezoid polymers. In conjunction with this, there is a gradual change into aromatic trapezoid structures.

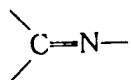
From Fig.2, it is possible to see that, as far as samples are concerned, in an air atmosphere and 195°C conditions-- following along with lengthening of heating periods--diffraction strengths associated with (100) peaks and (110) peaks decrease. Moreover, half peak widths are slightly narrowed before 30 minutes heating. This clearly shows that fiber molecular bonds have a tendency toward ordering, making trends toward serial pattern orderliness irregularities decrease. However, after 30 minutes, half peak widths get wider. Moreover, at $2\theta=24.78^\circ$ locations, the (101) peaks which present themselves are more and more obvious. This indicates that the original serial pattern structures are gradually destroyed and new serial pattern structures are gradually formed. As a result, it is possible to recognize that (101) peaks are the results of cyclization structures formed by molecules inside fiber samples during pyrolysis periods gradually being accumulated.

From Fig.2, it can also be seen that the peak positions of (100) diffraction peaks are also displaced from low angles toward high angles. However, the numerical values of translation (2θ) only lie between 16.16° and 16.33° . This type of tiny change is difficult to get to in discontinuous optical spectrum measurements associated with general X ray diffraction. It not only reflects the heating and mechanical histories undergone by fibers, it is also related to fiber high polymer structures and forms. In particular, alterations in internal stresses existing in samples due to pyrolysis conditions lead to there being displacements in diffraction line locations.

At 220°C and 235°C respectively, in the same way, locations with heating of 50 minutes and samples at $2\theta=24.78^\circ$ show the appearance of a new diffraction peak (omitted from charts). The diffraction strengths follow along with time periods, and the speed of increases are faster than when temperatures are 195°C . The explanation is that, at this time, cyclization structural accumulation serial patterns are clearer than when temperatures are 195°C . Moreover, (100) peak diffraction strengths are clearly weaker than when temperatures are 195°C . Half peak widths also increase. At the same time, (110) characteristic diffraction peaks gradually disappear. These phenomena mean that nitrile radicals in fiber molecules give rise to reactions, and the higher thermal processing temperatures are, the faster reaction speeds are.

Fig.3 shows X ray diffraction strength curves associated with different constant temperature time periods at 250°C . It is possible to clearly see that, following along with extensions of heating time periods, the patterns of change associated with various diffraction peaks--although similar to times when various temperatures discussed above applied--are, however, such that (100) peak

diffraction strengths drop even more severely. (110) peaks have already basically disappeared. Moreover, (101) peaks follow the trend toward increasing time periods and are clearer than at times when temperatures were 235°C. This experimental fact is in line with [10] the results--reported in previous articles--for the primary roles between PAN molecules during thermal stabilization processes and the determination of unceasing decreases in the ordered arrangements of $-C\equiv N$ radicals and gradual increases in conjugate nitrile radicals



2. Influences of Given Temperatures and Constant Temperature Time Periods on PAN Fiber Structure Parameters

On the basis of the contributions of crystal grain sizes to X ray diffraction peak widths--when not considering other factors giving rise to the widening of diffraction peaks--we adhere to P. Scherrer's empirical formulae [11]. Going through self-writing programs, micro computers calculate out half peak widths for (100) diffraction peaks in various charts. Taking Scherrer's constant to be 0.89, use is made of half height and width methods to directly solve for sample microcrystalline sizes (see Table 1) under different temperature and constant temperature time period conditions. At the same time, we also opt for the use of methods given by Reference [12] to carry out calculations of crystallinity in the sample in question under different temperature and constant temperature time period conditions. The results are also set out in Table 1.

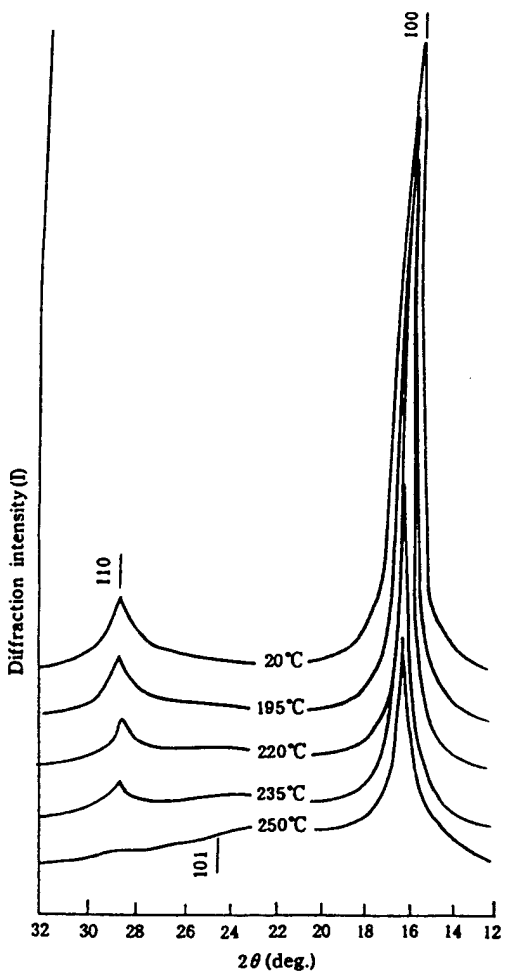


Fig. 1 Serial patterns of X-ray diffraction for a variation of the sample with temperature in air atmosphere

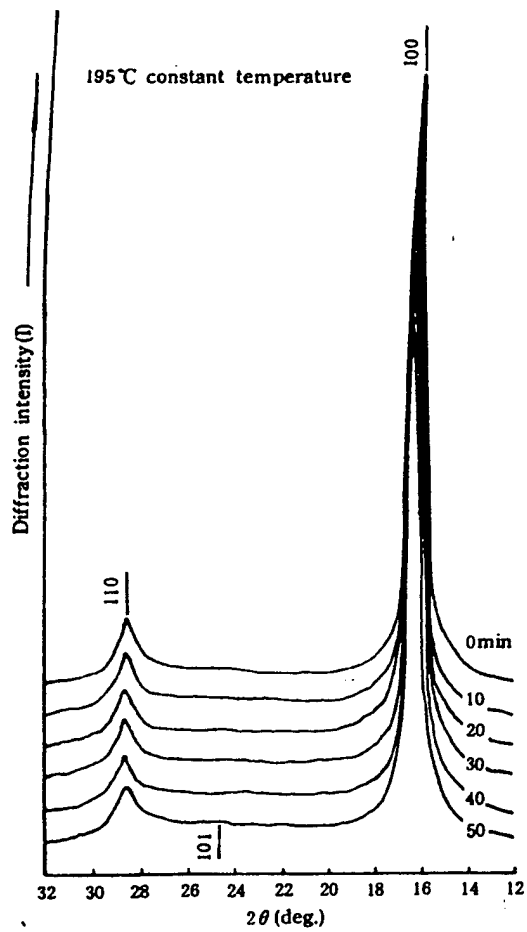


Fig. 2 X-ray diffraction profiles of the sample pyrolyzed under different times of constant temperature at 195°C

/552

(Tab.1)

Tab. 1 The microcrystalline size and the degree of crystallinity of PAN fibers
at the different temperatures and various times of constant temperature

Temp. (°C)	195		220		235		250	
	Micro- crystalline size (nm)	degree of crystallinity (%)						
0	13.24	50.24	11.87	46.85	9.46	34.34	9.93	17.83
10	13.23	49.75	10.18	35.54	7.23	21.98	6.62	8.51
20	13.23	49.84	9.93	29.99	6.62	17.53	4.97	5.93
30	12.43	45.45	9.69	25.82	6.11	14.35	4.41	3.93
40	12.04	45.85	9.24	22.51	5.68	13.03	3.97	3.69
50	11.68	45.48	8.82	19.87	4.97	10.56	3.31	2.48

From Table 1, it is possible to know that, following along with rises in thermal processing temperatures, sample microcrystalline sizes gradually become smaller, and drops in crystallinity become more acute. In accordance with the viewpoints of Minagawa and others [13], there are relationships between chemical reactions and polymerized patterns inside molecules. Therefore, during heat stabilization processes, PAN fiber chemical reactions show up first of all in areas of low ordering and gradually develop toward areas of high ordering. This indicates that preoxidation reactions carried out on the peripheries of ordered areas cause the rearranging of interstitial atoms, which leads to drops in the average sizes associated with these zones. Under the experimental conditions in question, the higher temperatures are, the faster reactions are carried out, determining that ordered structural arrangements of $C\equiv N$ radicals decrease even faster, making changes in microcrystalline sizes even more maximized.

/553

At the same time, from Table 1, one can also obviously see that, following along with extensions of pyrolysis periods, at 195°C, the two structural parameters in question fluctuate somewhat. However, the changes are not too great. Even so, after 220°C, microcrystalline sizes and crystallinities quite obviously follow changes in pyrolysis time periods. This clearly shows that ordered structural conditions associated with fiber atoms have been very greatly altered. Moreover, this type of structural change is not instantaneously completed. It goes through a process, that is, following along with the carrying out of reactions, hydrogen bonds in PAN molecules gradually meet destruction. The original ordered arrangements between molecules determined by hydrogen bonds also gradually meet

with destruction thereby leading to the obvious decreases in the two values discussed above.

Based on the aromatization index (AI) defined by Uchida and others [14], we used the sums and ratios of (101) peak diffraction strengths and (101) peak diffraction strengths plus (100) peak diffraction strengths, obtaining aromatization indices for samples under various experimental conditions. Fig.4 shows the influences of pyrolysis time periods on aromatization indices at different temperatures.

From Fig.4, it can be seen that, at the different temperatures in the experiments in question, when fiber samples are pyrolyzed--due to aromatization given rise to in the molecules of samples by preoxidation reactions--the aromatization indices all show a linear relationship to pyrolysis time periods. However, when samples are pyrolyzed at 195°C, 220°C, and 235°C, the aromatization indices follow pyrolysis time periods and slowly increase. It is only that the latter increases somewhat faster than the former, clearly showing that, in this time period, the production of condensed aromatic rings is still not too great. However, at 250°C, aromatization indices follow pyrolysis time periods and rapidly increase. This clearly shows that the speed of formation of condensed aromatic rings very, very greatly increases, causing the linear structure of the fibers in question to turn into a similar trapezoidal polymer structure [15] of segmented form with relatively high heat resistance properties.

From Fig.4, it is possible to know that, under 195°C constant temperature conditions, the crystal lattice spacing of samples (d100) cannot be seen to show any change. However, under constant temperature conditions of 220°C and 250°C, the lattice spacings all show dropping phenomena

after 10 minutes. Moreover, after constant temperatures for 20 minutes at 220°C, they have basically stabilized. However, under constant temperature conditions at 250°C, the d_{100} values still continuously drop. This may possibly be due to the consequences of a lattice distortion occurring in a crystal grain or between crystal grains.

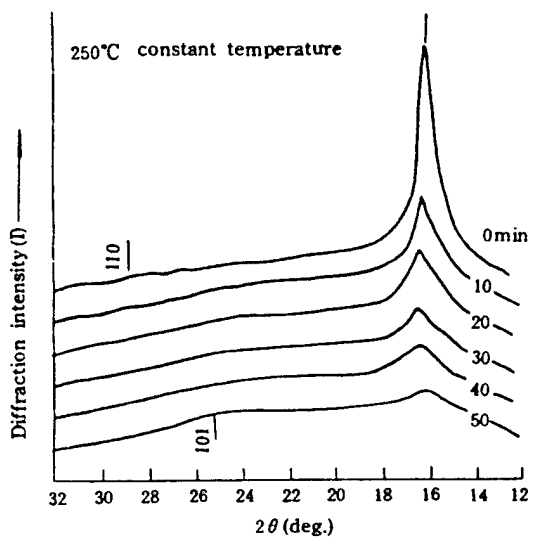


Fig. 3 X-ray diffraction profiles of the sample pyrolyzed under different times of constant temperature at 250°C

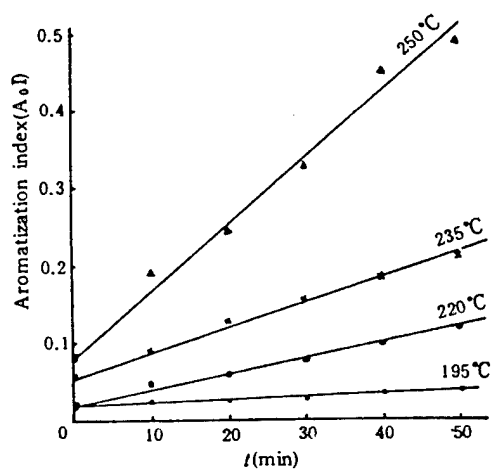


Fig. 4 Relationship between an aromatization index and the pyrolytic time when PAN fibers pyrolyzed at different temperatures

Aromatization index ($A_o I$)
time (min)

3. Calculations of Activation Parameters Associated with Cyclization Kinetics

Based on changes in fiber structure given rise to by chemical reactions, we returned to the consistency of structural destruction and the formation of new structures in terms of reaction kinetics, using (101) diffraction peaks to act as newly formed aromatization structures. Based on the fact that, at any instant, reaction speeds are only related to the amount of matter in question existing at that time, we were then able to go through a full linear analysis of temperature change spectra, solving for cyclization speed constants K for 195°C, 220°C, 235°C, and 250°C, which were, respectively, $1.63 \times 10^{-3} \text{ sec}^{-1}$; $2.43 \times 10^{-3} \text{ sec}^{-1}$; $3.82 \times 10^{-3} \text{ sec}^{-1}$; and, $4.63 \times 10^{-3} \text{ sec}^{-1}$. Following that, in accordance with Arrhenius theories, that is, $\ln K = \ln A - E/RT$, the symbols had normal meanings. Taking $\ln K$ and making a graph versus $1/T$, one obtains a linear relationship (such as that shown in Fig.6). From the slope of the straight line in Fig.6, one obtains the activation parameters for cyclization reactions of samples as 95.5966 kilojoules/mol.

Summarizing what has been described above, in order to understand PAN fiber dynamic pyrolysis characteristics and transient structural changes, in situ X ray diffraction techniques supplied adequate and reliable data as well as kinetics behavior related to cyclization reactions in molecules. Thus, important scientific information was given for optimized control in production and test manufacture of high performance PAN radical carbon fibers during thermal stabilization processes.

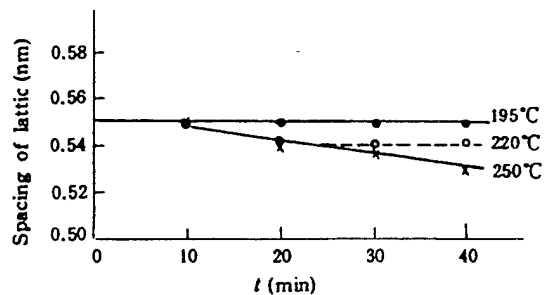


Fig. 5 Relationship between the spacing of lattice (d_{100}) for sample and the pyrolytic time at different temperatures

Spacing of latic (nm)
time(min)

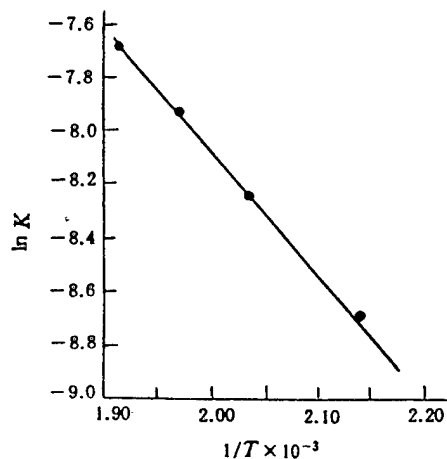


Fig. 6 Relationship between $\ln K$ and $1/T$

$\ln K$
 $1/T \times 10^{-3}$

ACKNOWLEDGEMENTS The samples used in this work were supplied by the Jilin chemical industry company reagent plant.

REFERENCES

- [1] Collins, G. L., Thomas, N. W., Williams, G. E., *Carbon*, 1988,26,671
- [2] Raskovic, V., Marinkovic, *Carbon*, 1975,13,535
- [3] Mun-Soo Lee, Keizo Miyasaka, 纤维学会志, 1990,46,263
- [4] Warner, S. B., Peebles, L. H., Uhlmann, D. R., *J. Mater. Sci.*, 1979,14,565
- [5] 胡恒亮、穆祥祺, X-射线衍射技术, 纺织工业出版社, 1988, P. 43
- [6] Wegener, W., Merkle, R., *Ges. Z., Textile Industrie*, 1971,73,303
- [7] Gupta, A. K., Chand, N., *Eur. Polym. J.*, 1979,15,899
- [8] Bohn, C. R., Schaeffgen, J. R., Statton, W. O., *J. Polym. Sci.*, 1961,55,531
- [9] Warner, S. B., Uhlmann, D. R., *J. Mater. Sci.*, 1979,14,1893
- [10] 赵根祥、陈邦杰, 应用科学学报, 1988,6,3,278
- [11] Debye, P., Scherrer, P., *Physik. Z.*, 1917,18,291
- [12] Alexander, L. E., "X-Ray Diffraction Methods In Polymer Science", Wiley-Interscience, New York, 1969, p. 167-168
- [13] Minagawa, M., Okamoto, M., Ishizuka, O., *J. Polym. Sci., Polym. Chem. Edition*, 1978,16,11,3031
- [14] Uchida, T., Shinoyama, I., Ito, Y., Nukuda, K., Proc. of the 10TH Bienn. Conf. on Carbon, Bethlechem, PA, 1971, p. 31
- [15] Gupta, A. K., Singhal, R. P., *J. Polym. Sci., Polym. Phys. Ed.*, 1983,21,2243

DISTRIBUTION LIST

DISTRIBUTION DIRECT TO RECIPIENT

<u>ORGANIZATION</u>	<u>MICROFICHE</u>
B085 DIA/RTS-2FI	1
C509 BALLOC509 BALLISTIC RES LAB	1
C510 R&T LABS/AVEADCOM	1
C513 ARRADCOM	1
C535 AVRADCOM/TSARCOM	1
C539 TRASANA	1
Q592 FSTC	4
Q619 MSIC REDSTONE	1
Q008 NTIC	1
Q043 AFMIC-IS	1
E404 AEDC/DOF	1
E410 AFDTC/IN	1
E429 SD/IND	1
P005 DOE/ISA/DDI	1
1051 AFIT/LDE	1
PO90 NSA/CDB	1

Microfiche Nbr: FTD95C000655
NAIC-ID(RS)T-0278-95